Ferdowsi University of Mashhad

I C C K E

International Conference on Computer and Knowledge Engineering

CERTIFICATE OF PRESENTATION

It is certified that

S. Etemadi, **M. Saadatmand-Tarzjan**, **M. Shamirzaei**, **J. Khosravi**,

Presented a paper titled

An Efficient 3D Gradient-Based Algorithm for Medical Image Registration Using Correlation-Coefficient Maximization

during the 4th International Conference on Computer and Knowledge Engineering (ICCKE 2014), held on October 29-30, 2014 at Ferdowsi University of Mashhad.

Seyed Amin Hosseini Seno, PhD

ICCKE 2014 Conference Chair

ICCKE 2014-336

An Efficient 3D Gradient-Based Algorithm for Medical Image Registration Using Correlation-Coefficient Maximization

S. Etemadi, M. Saadatmand-Tarzjan
Medical Imaging Lab, Department of Electrical Engineering
Ferdowsi University of Mashhad
Mashhad, Iran
shabnam.etemadi@stu.um.ac.ir,
saadatmand@um.ac.ir

M. Shamirzaei
Astronautics Research Institute
Iranian Space Research Center
Tehran, Iran
emumuc@yahoo.com

J. Khosravi
Department of Electrical Engineering
Shahid Rajaee Teacher Training University
Tehran, Iran
javanshir.khosravi@gmail.com

***Abstract*—Most registration algorithms for medical images may suffer from slow convergence and sensitivity to initialization. In this paper, we propose an efficient gradient-based algorithm for rigid intensity-based registration of medical images. It takes advantage of gradient-descend approach for maximizing the correlation coefficient similarity measure. Furthermore, we automatically adjust the optimization rate of algorithm for weak local minima avoidance and convergence acceleration. Experimental results demonstrated superior performance of the proposed algorithm compared to Powell's method (as a non-gradient algorithm) in terms of CPU time and solution quality for two sets of medical images.**

Keywords- Medical Image Registration; Correlation Coefficient; Rigid Transformation; Gradient-Based Optimization.

I. INTRODUCTION

Image registration is the process of aligning images to relate corresponding features. The images might be acquired with different imaging modals (*e.g.* MRI and CT) or the same modal at different times. Medical image registration plays an important role in disease diagnosis, treatment planning, and image-guided radiotherapy and surgery [1].

Two images or two sets of images are involved in a registration algorithm: the source/moving image $g(\boldsymbol{x}):\Omega\rightarrow\mathrm{R}$ and the fixed/reference image $f(\boldsymbol{x}):\Omega\rightarrow\mathrm{R}$ where $x\in\Omega$ represents a position in the n-dimensional domain Ω. The registration process is treated as an optimization algorithm which obtains the best transformation model T by maximizing the similarity between the fixed image (*i.e.* $f(\boldsymbol{x})$) and aligned moving image (*i.e.* $g(T(\boldsymbol{x}))$). Therefore, a typical registration algorithm consists of four components: transformation model, similarity measure, optimization framework, and interpolation method.

Transformation models of registration algorithms can be divided into two separate categories: rigid and non-rigid models. A rigid model can be entirely formulated by a few parameters since it is obtained by combination of a few primary transformations such as translation, rotation, scaling, and skew. In contrast, a non-rigid transformation is defined by the set of 2D/3D functions of a vector field [2]. Generally speaking, rigid transformation models are proper for global alignment while local registration is achieved only by using non-rigid models. Hereafter, we focus on the first category because the proposed registration algorithm works only with rigid transformation models.

Rigid registration algorithms can be separated into feature-based and intensity-based categories. Each feature-based registration algorithm primarily extracts some special robust features from every image. Then, by using corresponding features in the fixed and moving images, the optimal parameters of the transformation model are approximated. Feature-based registration algorithms usually require user interaction for significant sensitivity to noise, intensity variations, and imaging modality [3]. However, intensity-based registration algorithms optimize parameters of the transformation model by maximizing the similarity between intensities of pixels of the fixed and moving images [4]. Thus, they may provide better results especially for multimodal medical images because of robustness against noise, artifact, and intensity inhomogeneity.

Every intensity-based rigid registration algorithm takes advantage of an optimization algorithm to adjust the transformation parameters by maximizing (minimizing) a special similarity measure (cost function). A number of researchers preferred to use a non-gradient optimization algorithm, such as Powell's method [5], in the registration framework [6-8]. Non-gradient optimization algorithms provide a unique registration approach for all possible similarity measures. For example, Powell's method maximizes the similarity measure by using a bi-directional search along each transformation parameter. However, every registration algorithm with a non-gradient optimization method usually suffers from slow convergence and sensitivity to initialization (initial values of the transformation parameters). In contrast, although gradient-based optimization methods require analytical computation of derivatives of the similarity measure, they are more efficient and insensitive to initialization [9, 10].

Until now, researchers used a number of similarity measures (objective functions) with registration applications including least mean square errors, cross correlation, ratio image uniformity, mutual information (MI), and normalized mutual information (NMI) [7, 8]. It was shown that although cross correlation measure provides suitable solutions for registration of monomodal

978-1-4799-5487-2/14/$31.00 ©2014 IEEE

medical images, MI and NMI are preferred for multimodal medical images [11].

In this paper, an efficient gradient-based method is suggested for medical image registration. It employs the gradient-descend method to maximize the correlation-coefficient (CC) similarity measure. Furthermore, the optimization rate is effectively adjusted during algorithm convergence for local minima avoidance and registration acceleration. Experimental results demonstrated the superiority of the proposed algorithm over Powell's method in terms of CPU time and solution quality for two sets of medical images.

The reminder of this paper is organized as follows. In section II, we give an overview of rigid transformations. Principles of the proposed algorithm are provided in section III. Experimental results are presented in section IV and finally, section V is devoted to conclusion remarks.

II. RIGID TRANSFORMATIONS

A 3D linear transformation can be represented by multiplication of a matrix of size 4×4 to the pixel coordinates in the homogeneous space as follows:

$$\hat{\boldsymbol{x}} = T\boldsymbol{x} = \begin{bmatrix} t_{11} & t_{12} & t_{13} & t_{14} \\ t_{21} & t_{22} & t_{23} & t_{24} \\ t_{31} & t_{32} & t_{33} & t_{34} \\ 0 & 0 & 0 & 1 \end{bmatrix} \times \begin{bmatrix} x \\ y \\ z \\ 1 \end{bmatrix} = \begin{bmatrix} t_{11}x + t_{12}y + t_{13}z + t_{14} \\ t_{21}x + t_{22}y + t_{23}z + t_{24} \\ t_{31}x + t_{32}y + t_{33}z + t_{34} \\ 1 \end{bmatrix} \tag{1}$$

Where $\hat{\boldsymbol{x}} = [\hat{x}, \hat{y}, \hat{z}]^T$. In more detail, the 3D coordinates of a pixel can be represented in the 4D homogeneous space by setting the 4th dimension value to one.

All well-known linear transformations are obtained by combining the basic geometric transformations including translation, rotation, scaling, skew, and perspective. For example, rigid-body transformation is given by combining a translation and 3 rotation transformations as follows:

$$T_{rigid-body} = \begin{bmatrix} \cos\beta\cos\theta & \cos\beta\sin\theta\cos\alpha - \sin\alpha\sin\beta & \cos\beta\sin\theta\sin\alpha + \sin\beta\cos\alpha & t_x \\ -\sin\theta & \cos\theta\cos\alpha & \cos\theta\sin\alpha & t_y \\ -\sin\beta\cos\theta & -\sin\beta\sin\theta\cos\alpha - \sin\alpha\cos\beta & -\sin\beta\sin\theta\sin\alpha + \cos\beta\cos\alpha & t_z \\ 0 & 0 & 0 & 1 \end{bmatrix} \tag{2}$$

Where α, β and θ (t_x, t_y, and t_z) indicate the rotation angles around (translation parameters along) the x, y and z axes, respectively. Another example is affine transformation which consists of all basic geometric transformations except perspective. It can be formulated by:

$$T_{affine} = \begin{bmatrix} \eta_x \cos\beta\cos\theta & s_{xy}(\cos\beta\sin\theta\cos\alpha - \sin\alpha\sin\beta) & s_{xz}(\cos\beta\sin\theta\sin\alpha + \sin\beta\cos\alpha) & t_x \\ -s_{xy}\sin\theta & \eta_y\cos\theta\cos\alpha & s_{yz}\cos\theta\sin\alpha & t_y \\ -s_{xz}\sin\beta\cos\theta & -s_{yz}(\sin\beta\sin\theta\cos\alpha + \sin\alpha\cos\beta) & \eta_z(-\sin\beta\sin\theta\sin\alpha + \cos\beta\cos\alpha) & t_z \\ 0 & 0 & 0 & 1 \end{bmatrix} \tag{3}$$

Where η_x, η_y and η_z denote the scaling parameters along x, y and z axes, respectively; and s_{xy}, s_{zy} and s_{xz} are skew parameters.

III. PROPOSED ALGORITHM PRINCIPLES

In the proposed scheme, we employ gradient descent, which is a first-order optimization algorithm, for easy implementation and convergence guarantee.

A. Optimization algorithm

Let's the vector $\boldsymbol{p}$ includes all transformation parameters. For example, for the affine transformation of Eqn. (3), we can write:

$$\boldsymbol{p}_{affine} = [\alpha \quad \beta \quad \theta \quad t_x \quad t_y \quad t_z \quad \eta_x \quad \eta_y \quad \eta_z \quad s_{xy} \quad s_{xz} \quad s_{yz}]^T \tag{4}$$

According to the gradient descend algorithm, a local maximum of the similarity measure c can be obtained by solving the following numerical equation:

$$\boldsymbol{p}^{k+1} = \boldsymbol{p}^k + \lambda \nabla c \tag{5}$$

Where λ represents the optimization rate and ∇ denotes the gradient operator (*i.e.* $\nabla c = \partial c / \partial \boldsymbol{p}$).

However, gradient descend suffers from slow convergence and getting caught in weak local minima. Although second-order optimization algorithms such as Newton and Levenberg-Marquardt may provide better solutions, they require the second-order derivatives for implementation and may diverge away from nearby local optima.

On the other hand, we can improve the performance of the gradient descend algorithm by appropriate regulation of λ. Yam and Chow's algorithm [12] proposed an effective method for adjusting the learning rate of feed-forward neural networks. This method modifies the learning rate in accordance with the correlation between two consecutive gradient vectors. In this case, three different conditions may be occurred:

1) When the correlation coefficient is near to one, there is almost no change in the directions of gradient vectors. Thus, the convergence rate (λ) can be increased.

2) Once the correlation coefficient is near to minus one, the gradient vectors are almost in the opposite direction. Hence, λ should be reduced to lessen oscillations of parameters values during convergence.

3) When there is no correlation between two consecutive gradient vectors, λ remains constant.

They showed that with the above regulation process, the number of iterations of gradient-descend was a little larger than that of Levenberg-Marquardt while its computational burden is significantly better.

B. Similarity measure

We choose the correlation coefficient (CC) as the similarity measure of the proposed registration algorithm. Suppose that n sample pixels (*i.e.* $\boldsymbol{x}_i \in \Omega$, i=1,2,…,n) have been chosen from the domain of $g(\boldsymbol{x})$. By definition, the correlation coefficient between the fixed image and moving image is given by:

$$c_{CC} = \frac{\sum_{i=0}^{n-1}\left(g(T\boldsymbol{x}_i)-\mu_g\right)\left(f(\boldsymbol{x}_i)-\mu_f\right)}{\hat{\sigma}_g\hat{\sigma}_f} \tag{6}$$

Where μ_g and μ_f represent the average intensities of the moving and fixed images as follows:

$$\begin{cases}\mu_g = \frac{1}{n}\sum_{i=0}^{n-1} g(T\boldsymbol{x}_i) \\ \mu_f = \frac{1}{n}\sum_{i=0}^{n-1} f(\boldsymbol{x}_i)\end{cases} \tag{7}$$

Furthermore, $\hat{\sigma}_g$ and $\hat{\sigma}_f$ are related to the standard deviations of intensities of the moving and fixed images, given by:

$$\begin{cases}\hat{\sigma}_g = \sqrt{\sum_{i=0}^{n-1}(g(T\boldsymbol{x}_i)-\mu_g)^2} \\ \hat{\sigma}_f = \sqrt{\sum_{i=0}^{n-1}(f(\boldsymbol{x}_i)-\mu_f)^2}\end{cases} \tag{8}$$

The CC value is always in the range [-1,1]. Obviously, by increasing similarity between intensity distributions of the fixed and moving images, CC approaches to 1 and vice versa.

According to Eqn. (5), ∇c_{CC} should be computed for to implementation of the gradient descend algorithm. Thus, we can write:

$$\begin{aligned}\nabla c_{CC} &= \frac{\partial c_{CC}}{\partial \mathbf{p}} \\ &= \frac{\left[\frac{\partial}{\partial \mathbf{p}}\sum_{i=0}^{n-1}\left(g(T\mathbf{x}_i)-\mu_g\right)\left(f(\mathbf{x}_i)-\mu_f\right)\right]\hat{\sigma}_g\hat{\sigma}_f}{\hat{\sigma}_g{}^2\hat{\sigma}_f{}^2} \\ &\quad - \frac{\left[\frac{\partial\hat{\sigma}_g}{\partial \mathbf{p}}\right]\hat{\sigma}_f\sum_{i=0}^{n-1}\left(g(T\mathbf{x}_i)-\mu_g\right)\left(f(\mathbf{x}_i)-\mu_f\right)}{\hat{\sigma}_g{}^2\hat{\sigma}_f{}^2} \\ &= \frac{\frac{\partial}{\partial \mathbf{p}}\sum_{i=0}^{n-1}\left(g(T\mathbf{x}_i)-\mu_g\right)\left(f(\mathbf{x}_i)-\mu_f\right)}{\hat{\sigma}_g\hat{\sigma}_f} - \frac{c_{CC}}{\hat{\sigma}_g}\frac{\partial\hat{\sigma}_g}{\partial \mathbf{p}}\end{aligned} \tag{9}$$

The first term of the above equation can be further simplified as follows:

$$\begin{aligned}&\frac{\partial}{\partial \mathbf{p}}\sum_{i=0}^{n-1}\left(g(T\mathbf{x}_i)-\mu_g\right)\left(f(\mathbf{x}_i)-\mu_f\right) \\ &= \sum_{i=0}^{n-1}\left(f(\mathbf{x}_i)-\mu_f\right)\frac{\partial}{\partial \mathbf{p}}\left(g(T\mathbf{x}_i)-\mu_g\right) \\ &= \sum_{i=0}^{n-1}\left(f(\mathbf{x}_i)-\mu_f\right)J\nabla g(T\mathbf{x}_i) - \underbrace{\left[\sum_{i=0}^{n-1}\left(f(\mathbf{x}_i)-\mu_f\right)\right]}_{0}\frac{\partial\mu_g}{\partial \mathbf{p}} \\ &= \sum_{i=0}^{n-1}\left(f(\mathbf{x}_i)-\mu_f\right)J\nabla g(T\mathbf{x}_i)\end{aligned} \tag{10}$$

Where $\nabla g(T\mathbf{x}_i) = \left.\frac{\partial g(\mathbf{x})}{\partial \mathbf{x}}\right|_{\mathbf{x}=T\mathbf{x}_i}$ and the Jacobean matrix J is given by:

$$J = \frac{\partial T\boldsymbol{x}}{\partial \boldsymbol{p}} = \frac{\partial \hat{\boldsymbol{x}}}{\partial \boldsymbol{p}} \tag{11}$$

For example, the Jacobean matrix of the affine transformation (Eqn. 3) can be computed as follows:

$$J_{affine} = \begin{bmatrix} \frac{\partial\hat{x}}{\partial\alpha} & \frac{\partial\hat{y}}{\partial\alpha} & \frac{\partial\hat{z}}{\partial\alpha} \\ \frac{\partial\hat{x}}{\partial\beta} & \frac{\partial\hat{y}}{\partial\beta} & \frac{\partial\hat{z}}{\partial\beta} \\ \vdots & \vdots & \vdots \\ \frac{\partial\hat{x}}{\partial s_{yz}} & \frac{\partial\hat{y}}{\partial s_{yz}} & \frac{\partial\hat{z}}{\partial s_{yz}} \end{bmatrix} \tag{12}$$

In the same manner, the second term of Eqn. (9) can be simplified as follows:

$$\begin{aligned}\frac{\partial\hat{\sigma}_g}{\partial \mathbf{p}} &= \frac{\partial}{\partial \mathbf{p}}\sqrt{\sum_{i=0}^{n-1}\left(g(T\mathbf{x}_i)-\mu_g\right)^2} \\ &= \frac{1}{2}\frac{\frac{\partial}{\partial \mathbf{p}}\sum_{i=0}^{n-1}\left(g(T\mathbf{x}_i)-\mu_g\right)^2}{\sqrt{\sum_{i=0}^{n-1}\left(g(T\mathbf{x}_i)-\mu_g\right)^2}} \\ &= \frac{1}{\hat{\sigma}_g}\sum_{i=0}^{n-1}\left(g(T\mathbf{x}_i)-\mu_g\right)\frac{\partial}{\partial \mathbf{p}}\left(g(T\mathbf{x}_i)-\mu_g\right) \\ &= \frac{1}{\hat{\sigma}_g}\sum_{i=0}^{n-1}\left(g(T\mathbf{x}_i)-\mu_g\right)J\times\nabla g(T\mathbf{x}_i) - \frac{\partial\mu_g}{\partial \mathbf{p}}\underbrace{\sum_{i=0}^{n-1}\left(g(T\mathbf{x}_i)-\mu_g\right)}_{0} \\ &= \frac{1}{\hat{\sigma}_g}\sum_{i=0}^{n-1}\left(g(T\mathbf{x}_i)-\mu_g\right)J\times\nabla g(T\mathbf{x}_i)\end{aligned} \tag{13}$$

Finally, by inserting Eqns. (10) and (13) in Eqn. (9), ∇c_{CC} can be computed as follows:

$$\nabla c_{CC} = \sum_{i=0}^{n-1} w_{CC}(\boldsymbol{x}_i, T)\, J\nabla g(T\boldsymbol{x}_i) \tag{14}$$

Where the weighting coefficient $w_{CC}(x_i,T)$ is given by:

$$w_{CC}(\mathbf{x}_i;T) = \frac{1}{\hat{\sigma}_g}\left(\frac{f(\mathbf{x}_i)-\mu_f}{\hat{\sigma}_f} - c_{CC}\frac{g(T\mathbf{x}_i)-\mu_g}{\hat{\sigma}_g}\right) \tag{15}$$

TABLE I. COMPARING THE SPATIAL ACCURACY OF THE PROPOSED GRADIENT-BASED ALGORITHM AND POWELL'S METHOD FOR THREE PAIRS OF 3D CT IMAGES OF THE HUMAN CHEST. THE BEST RESULTS HAVE BEEN INDICATED BY BOLD-FACE TEXT.

Benchmark Images	Proposed Method (Average ± STD)	Powell's Method (Average ± STD)
1st Pair	**2.6951**±1.4438	3.9451 ±2.3772
2nd Pair	**3.2207**±1.9780	3.8197 ±2.4299
3rd Pair	**4.5396**±2.9831	6.3778 ±3.8745
Total	**3.4851** ±2.3573	4.7142 ±3.1975

TABLE II. COMPARING THE COEFFICIENTS OF THE DESIRED AFFINE TRANSFORMATION WITH THOSE OBTAINED BY THE PROPOSED ALGORITHM AND POWELL'S METHOD FOR THREE PAIRS OF 3D CT IMAGES OF THE HUMAN CHEST.

Benchmark Images	Desired Affine Transformation	Proposed Method	Powell's Method
1st Pair	$\begin{bmatrix} 0.9848 & -0.1736 & 0 & 11 \\ 0.1736 & 0.9848 & 0 & 11 \\ 0 & 0 & 1 & 11 \\ 0 & 0 & 0 & 1 \end{bmatrix}$	$\begin{bmatrix} 0.9853 & -0.1722 & 0 & 10.7644 \\ 0.1737 & 0.9833 & 0.0002 & 11.2033 \\ 0 & 0 & 1 & 10.9941 \\ 0 & 0 & 0 & 1 \end{bmatrix}$	$\begin{bmatrix} 0.9847 & -0.1729 & 0 & 12.7193 \\ 0.1739 & 0.9847 & 0 & 8.9450 \\ 0 & 0 & 0.9980 & 10.8792 \\ 0 & 0 & 0 & 1 \end{bmatrix}$
2nd Pair	$\begin{bmatrix} 0.9903 & -0.1392 & 0 & 11.0000 \\ 0.1392 & 0.9903 & 0 & 4.0640 \\ 0 & 0 & 1 & 3.0270 \\ 0 & 0 & 0 & 1 \end{bmatrix}$	$\begin{bmatrix} 0.9900 & -0.1393 & 0.0004 & 10.8504 \\ 0.1401 & 0.9898 & -0.0004 & 4.1817 \\ -0.0003 & 0.0005 & 1.0004 & 2.9893 \\ 0 & 0 & 0 & 1 \end{bmatrix}$	$\begin{bmatrix} 0.9916 & -0.1392 & 0 & 11.4670 \\ 0.1392 & 0.9906 & 0 & 2.5385 \\ 0 & 0 & 1 & 3.0430 \\ 0 & 0 & 0 & 1 \end{bmatrix}$
3rd Pair	$\begin{bmatrix} 1.2483 & 0.0068 & 0.0651 & 14.4531 \\ 0 & 0.9945 & -0.1450 & 5.1250 \\ -0.0523 & 0.1044 & 0.9932 & 7.9219 \\ 0 & 0 & 0 & 1.0000 \end{bmatrix}$	$\begin{bmatrix} 1.2423 & 0.0045 & 0.0455 & 15.7727 \\ 0.0021 & 0.9924 & -0.1374 & 4.5883 \\ -0.0558 & 0.1385 & 0.9961 & 6.4662 \\ 0 & 0 & 0 & 1 \end{bmatrix}$	$\begin{bmatrix} 0.7983 & 0.0019 & 0.0548 & 11.2824 \\ 0.0052 & 0.9870 & -0.1379 & 5.5177 \\ -0.0430 & 0.1372 & 0.9930 & 6.8176 \\ 0 & 0 & 0 & 1 \end{bmatrix}$

As shown, Eqn. (14) includes three separate terms. The weighting scalar w_{CC} computes the intensity difference between each pair of corresponding pixels in the fixed and moving images. The gradient vector $\nabla g(Tx)$ encodes intensity variations along each axis. Finally, the Jacobean matrix J relates spatially intensity variations to the transformation parameters.

In other words, w_{CC} is dependent to the similarity measure while J is completely indicated by the rigid transformation. For example, if we want to extend Eqn. (14) for rigid-body transformation (*i.e.* $\boldsymbol{p}_{rigid-body} = [\alpha \quad \beta \quad \theta \quad t_x \quad t_y \quad t_z \quad 1 \quad 1 \quad 1 \quad 1 \quad 1 \quad 1]^T$), it will be sufficient to recomputed the Jacobean matrix as follows:

$$J_{\text{rigid-body}} = \begin{bmatrix} \mathbf{1}_{6\times6} & \mathbf{0}_{6\times6} \\ \mathbf{0}_{6\times6} & \mathbf{0}_{6\times6} \end{bmatrix} \times J_{\text{affine}} \tag{16}$$

Where $\mathbf{1}_{6\times6}$ indicates an identity matrix of size 6×6.

IV. RESULTS

All experiments were performed in the MATLAB environment by using a LAPTOP with Intel Core i5 2.40GHz CPU and 4 GB main memory. We compared the performance of the proposed algorithm with Powell's method (implemented in the well-known frequently-used SPM toolkit for registration of 3D magnetic resonance brain images [13]) for two sets of benchmark images.

Expert landmark correspondences have become a widely adopted reference for evaluating medical image registration (MIR) spatial accuracy.

The expert-determined landmark features used to evaluate spatial accuracy in this study is the reference DIR-Lab[1] dataset [14]. The ongoing DIR-Lab web project consists of ten breath-hold computed tomography (BH-CT) image sets acquired from the National heart lung blood institute study archive. Each available image dataset has associated with a coordinates list of anatomical landmarks that have been manually identified and registered by an expert in thoracic imaging. The point sets serve as a reference for evaluating the spatial accuracy of registration within the lung for each case.

In the first set of benchmark images, three BH-CT image pairs were randomly selected from the DIR-Lab database. Then, each pair of images was registered by the proposed gradient-based algorithm and Powell's method. Finally, the mean and standard deviation (STD) of spatial Euclidean distances between the corresponding reference and registered landmark points were computed. As shown in Table I, for all benchmark images, the proposed algorithm outperformed Powell's method in terms of average spatial accuracy.

Furthermore, for each pair of benchmark images, the desired affine transformation is further compared with results of the proposed algorithm and Powell's method in Table II. Clearly, compared to Powell's method, the proposed algorithm could better approximate the coefficients of the affine transformation matrix. It is further illustrated in Table III in which the average proportional error of transformation matrix coefficients is reported for each pair of benchmark images. As shown, compared to Powell's method (with 23.12%), the proposed algorithm (with 8.64%), on average, enhanced the proportional error by at least 14%.

Figures 1-3 illustrate the registration results obtained by the proposed algorithm and Powell's method for three pairs of 3D magnetic resonance images of the human brain (*i.e.* the second set of benchmark images). These images were chosen from among the samples of the SPM toolkit [13]. As shown, despite initially significant mis-registrations between fixed and moving images, both of the counterpart methods (*i.e.* the proposed algorithm and Powell's method) were globally successful to register all the pairs of benchmark images. However, the proposed algorithm provided better spatial accuracy.

Finally, the average CPU time of the proposed algorithm was 36.2 seconds which was superior to that of Powell's method (with CPU time of 44.4 seconds) by at least 8 seconds (*i.e.* 20%).

[1] http://www.dir-lab.com

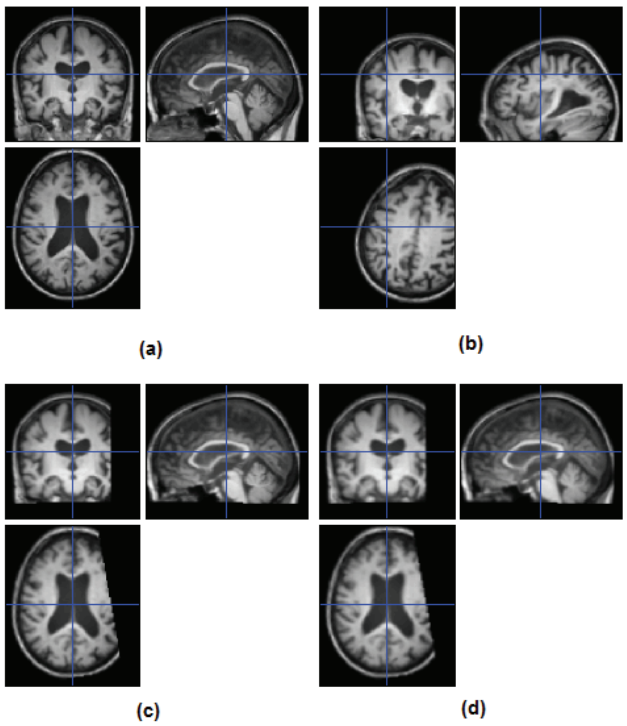

Figure 1. Comparing the results of the proposed algorithm with those of Powell's method for the first pair of benchmark images of the human brain: (a) three sample slices of the fixed image, (b) three corresponding slices of the moving image, (c) results of the proposed algorithm, and (d) results of Powell's method.

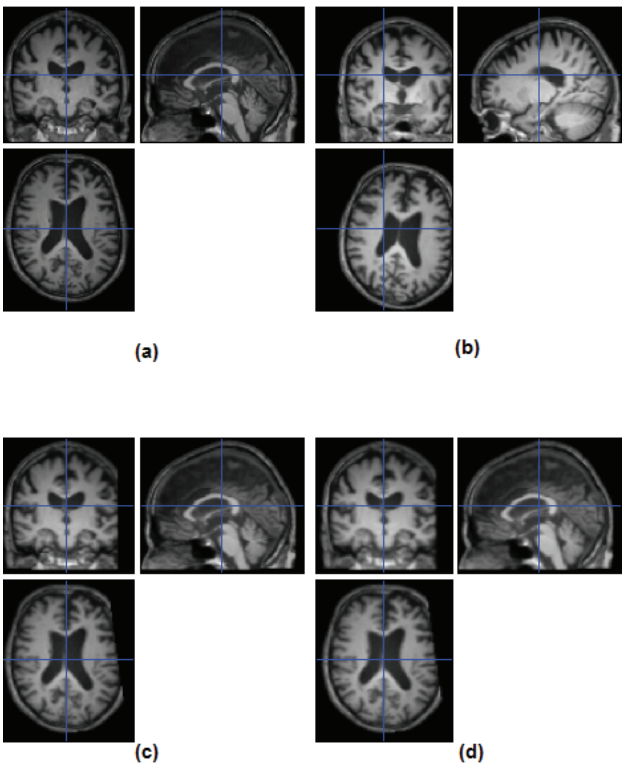

Figure 2. Comparing the results of the proposed algorithm with those of Powell's method for the second pair of benchmark images of the human brain: (a) three sample slices of the fixed image, (b) three corresponding slices of the moving image, (c) results of the proposed algorithm, and (d) results of Powell's method.

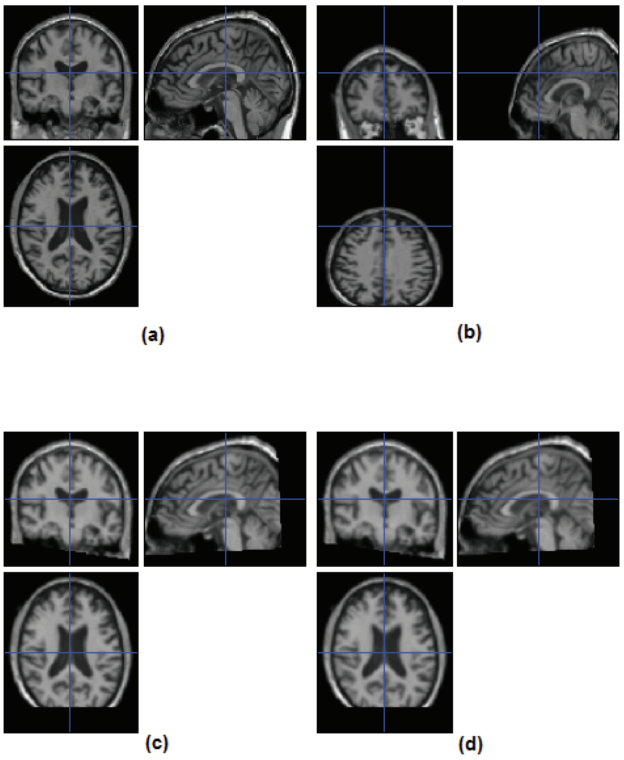

Figure 3. Comparing the results of the proposed algorithm with those of Powell's method for the third pair of benchmark images of the human brain: (a) three sample slices of the fixed image, (b) three corresponding slices of the moving image, (c) results of the proposed algorithm, and (d) results of Powell's method.

TABLE III. COMPARING THE AVERAGE (± STD) PROPORTIONAL ERROR OF THE AFFINE TRANSFORMATION COEFFICIENTS OF THE PROPOSED ALGORITHM WITH THOSE OF POWELL'S METHOD FOR THREE PAIRS OF 3D CT IMAGES OF THE HUMAN CHEST. THE BEST RESULTS HAVE BEEN INDICATED BY BOLD-FACE TEXT.

Benchmark Images	**Proposed Method** (Mean ± STD)	**Powell's method** (Mean ± STD)
1st Pair	**0.0280**±0.0750	0.2436 ±0.6452
2nd Pair	**0.0193**±0.0460	0.1256 ±0.3910
3rd Pair	**0.2120**±0.4783	0.3247 ±0.8142
Total	**0.0864**±0.2890	0.2313 ±0.6325

V. CONCLUSION

We have developed an efficient gradient-based algorithm for rigid intensity-based registration of medical images by maximizing the correlation coefficient similarity measure. For optimization of the transformation parameters, the gradient descend method is used. Moreover, we used Yam and Chow's method [12] to effectively adjust the optimization rate of the proposed algorithm for convergence acceleration and weak local minima avoidance.

It was shown that the proposed optimization formulation can be used with every rigid transformation by appropriately changing the Jacobean matrix.

Experimental results demonstrated the superior performance of the proposed algorithm compared to Powell's method in terms of both solution quality and CPU time for two sets of 3D medical images.

REFERENCES

[1] Joseph V. Hajnal, Derek L. G. Hill, and David J. Hawkes, "Medical image registration," 1st ed., CRC press LLC, 2001, pp. 12-136.

[2] A. Gholipour, N. Kehtarnavaz, R. Briggs, M. Devous, and K. Gopinath, "Brain functional localization: A survey of image registration techniques," IEEE Trans. Medical Imaging, vol. 26, pp. 427-451, 2007.

[3] Ho Lee, Jeongjin Lee, Namkug Kim, Sang J. Kim, and Yeong G. Shin, "Robust feature-based registration using a gaussian-weighted distance map and brain feature points for brain PET/CT images," Computers in Biology and Medicine, vol. 38, pp. 945-961, 2008.

[4] Andrea Valsecchi, Sergio Damas, José Santamaría, and Linda Marrakchi-Kacem, "Intensity-based image registration using scatter search," Artificial Intelligence in Medicine, vol. 60, pp. 151-163, 2014.

[5] M. J. D. Powell, "An efficient method for finding the minimum of a function of several variables without calculating derivatives," Computer Journal, vol. 7, pp. 155-162, 1964.

[6] Tharindu De Silva and et. al., "2D-3D rigid registration to compensate for prostate motion during 3D TRUS-guided biopsy," Medical Physics, vol. 40, pp. 1-13, 2013.

[7] J. P. W. Pluim, J. B. A. Maintz, and M. A. Viergever, "Mutual information based registration of medical images: A survey," IEEE Trans. Medical Imaging, vol. 22, pp. 986-1004, 2003.

[8] X. Xiaoyan, and R. D. Dony, "Differential evolution with Powell's direction set method in medical image registration," IEEE Int'l Sym. Biomedical Imaging: Nano to Macro, vol. 1, pp. 732-735, 2004.

[9] P. Markelj, D. Tomazevic, F. Pernus, and B. Likar, "Robust gradient-based 3D/2D registration of CT and MR to X-Ray images," IEEE Trans. Medical Imaging, vol. 27, pp. 1704-1714, 2008.

[10] T. Cheah, S. Shanmugam1, and K. Ang Li Mann, "Medical image registration by maximizing mutual information based on combination of intensity and gradient information," Int'l Conf. Biomedical Engineering, pp. 27-28, 2012.

[11] G. P. Penney and et. al., "A comparison of similarity measures for use in 2D, 3D medical image registration," IEEE Trans. Medical Imaging, vol. 17, pp. 586-595, 1998.

[12] J. Y. F. Yam, and T. W. S. Chow, "Extended least squares based algorithm for training feedforward networks," IEEE Trans. Neural Networks, vol. 8, pp. 806-810, 1997.

[13] K. J. Friston, J. Ashburner, S. J. Kiebel, T. E. Nicholas, and W. D. Penny, "Statistical parametric mapping: The analysis of functional brain images," 1st ed., Academic Press, 2006, pp. 40-50.

[14] R. Castillo and et. al., "A framework for evaluation of deformable image registration spatial accuracy using large landmark point sets," Phys. Med. Biol., vol. 54, pp. 1849-1870, 2009.